NWS/Hydrology

Laboratory

Technical Report

STATISTICAL COMPARISON OF MEAN AREAL PRECIPITATION ESTIMATES FROM WSR-88D, OPERATIONAL AND HISTORICAL GAGE NETWORKS

Dahong Wang
Michael B. Smith
Ziya Zhang
Victor I. Koren
Seann Reed
Hydrologic Research Laboratory
Office of Hydrology
National Weather Service/NOAA
1325 East-west Highway
Silver Spring, MD 20910
david.wang@noaa.gov
(301) 713-0640 x157

August 13, 2001

ABSTRACT

The mean areal precipitation (MAP) estimates derived using precipitation data from the River Forecast Center's (RFC) Weather Surveilance Radar 1988-Doppler (WSR-88D), RFC's operational gage network and National Climatic Data Center's (NCDC) historic gage network are statistically compared over the eight basins in Arkansas-Red River Basin. 6-hr radar-based MAP (MAPX), Operational MAP (MAPO) and historic MAP (MAPH) estimates in the period from June 1, 1993 to May 31, 1998 are computed by preprocessors at Hydrologic Research Laboratory (HRL). The MAPX values are derived from the gridded hourly NEXRAD stage III precipitation estimates before June 15, 1996 and thereafter from a mixed use of the stage III and P1 processing algorithms. In terms of long-term averages, MAPX are in very good agreement with MAPO and MAPH. The overall average ratio of 6-hr MAPX to MAPO value over the eight basins is 0.985, while the ratio of MAPH to MAPO is 0.974. However, the MAPX values are strongly dependent on the processing algorithms. The underestimation in a range of 3~6% was found for MAPX values with comparison of MAPO estimates before June 15, 1996 while the overestimation was noted for MAPX values after June 15, 1996. When radar and operational gages predicted the same amount of precipitation, the radar estimates tended to be more intense and less spread out. Effects of the three MAP estimates on SAC-SMA runoff output are also studied. Error statistics of three simulations reveal that percent bias of MAPX-forced simulation is –4.31, while percent biases of MAPO and MAPH-forced simulations are -11.72% and –8.79, respectively.

1. INTRODUCTION

The National Weather Service River Forecast System (NWSRFS) is a comprehensive set of models and hydrologic techniques used by the National Weather Service (NWS) River Forecast Centers (RFC) to conduct hydrologic forecasting. The Sacramento Soil Moisture Accounting (SAC-SMA) model (Burnash et al.,1973), which uses mean areal precipitation (MAP) input and outputs runoff, is an important component of the prediction program in the NWSRFS. Therefore, a detailed analysis of model input MAP is required to understand how these model inputs will affect model performance.

In the NWSRFS, the SAC-SMA is first calibrated from time series using historic MAP (MAPH) input, then the calibrated model parameters are used for real-time forecasting. Raw precipitation for deriving MAPH is retrieved from the National Climatic Data Center (NCDC) archives. In the operational forecast system, the SAC-SMA usually inputs time series of operational MAP (MAPO), which is derived from the RFC's operational observed network. Installation of an advanced system of radars called Weather Surveillance Radar 1988-Doppler (WSR88-D) (Hudlow, 1988) has provided opportunity to use radar-based MAP (MAPX) at a 4X4 km^2 spatial scale and a 1-hr time step. However, radar rainfall estimates are processed by taking the operational observed precipitation as "ground truth". Therefore, it is important to also evaluate operational observed data by comparing them with NCDC historic precipitation.

The advantages of using MAPX for SAC-SMA simulation over the Arkansas-Red Basin have been documented by Smith et al. (1999). They found that the MAPX-forced simulations performed better than the MAPO-forced simulations in runoff. Similar research has been done by Borga et al. (1998) on statistical analysis of radar rainfall and runoff simulation on six flood events for two medium size watersheds in northern Italy. The radar rainfall was found to preclude the more accurate simulation of runoff. However, there exist differences among MAPX , MAPO and MAPH. Finnerty and Johnson (1997) found that MAPX are biased low compared with MAPH over several basins near Tulsa, Okla. for a 7-month period. Stellman et al. (2000) found such biases changed seasonally and the radar underestimates precipitation amounts by as much as 50% over the Flint River Basin, GA during winter months.

Previous studies have compared radar estimates to gage estimates but there have been fewer studies dealing with MAPX, MAPO and MAPH. The estimation of rainfall for flood prediction from WSR-88D reflectivity over the region at Dickinson, TX, during 17-18 October 1994 was compared to rain gages by Vieux and Bedient (1998). In their study, the rainfall estimates from the WSR-88D reflectivity data with a Z-R relationship of $Z=250R^{1.2}$ are different from the daily gage rainfall estimates within 6% and 15% in amount for the two days investigated.

This work is aimed at providing insight for evaluating the SAC-SMA model performance when it is used to simulate river runoff with radar-based MAPX and gage MAP data. The study expands the work by Johnson et al. (1999) to better understand forcing

differences on simulations in a longer period. Insights gained from this study might be useful in developing tools and procedures to enable River Forecasting Center (RFC) personnel to more effectively use the NEXRAD data for short-term hydrologic forecasting. This paper describes a detailed analysis of model input MAPs from the WSR88-D radar data (MAPX), RFC's operational rain gage data (MAPO) and NCDC's historic rain gage data (MAPH), as well as effect of these MAPs on model performance.

2. STUDY BASINS AND DATA

Eight basins in the region near the Oklahoma-Arkansas-Missouri state boundaries, shown in Figure 1, are selected for this study. The basins in the study are generally in the foothills of the Ozark Mountains of NW Arkansas and SW Missouri. Rolling hills predominate with elevations generally ranging from 800 feet to 1500 feet. The highest elevations occur in the eastern most areas. Land use cover is a mix of forests and grasslands used for grazing, with forests increasing in amount as one moves to the east. The basins are generally rural in character with little in the way of any towns more than 2500 people. Rainfall is generally distributed well throughout the year with a slight maximum in the spring. Average annual rainfall is 40 to 45 inches. The rain gages used to compute the MAPO and MAPH data, and radar locations are also shown in Figure 1. The basin names and relevant geographic feature are provided with Table 1.

This region was analyzed because of its dense gage network, overlapping radar umbrellas, and one of the longest available periods of archived NEXRAD radar products in the United States. The study period is from June 1, 1993 to May 31, 1998. The rainfall data used to process 6-hr MAPO, 1-hr MAPH and 1-hr MAPX data for all eight0 basins during this period are archived at NWS Hydrologic Research Laboratory (HRL), Office of Hydrology.

Time series of MAPO data are derived from observed precipitation amounts measured by an operational network of precipitation gages in which the gages report at a variety of time steps, most commonly 1, 3, 6, and 24 hours. Rainfall reports from different gages are accumulated to derive daily totals. Missing data are estimated from surrounding gages using a $1/d^2$ weighting method. A daily MAPO is computed by using Thiessen polygon or other weighting schemes, then distributed into 6 hour periods based on the precipitation values of the recording gage closest to the centroid of the basin in each of 4 quadrants. Operational MAPO data are computed by the MAP operational preprocessor. The details of this operational procedure can be found in the National Weather Service (NWSRFC User's Manual, 1976).

Time series of MAPX data are calculated by simply averaging radar cell estimates within basins. MAPX data used for this study are derived from radar rainfall estimates generated by using two algorithms: Stage III or Process 1 (P1), based on radar data and rain gauge reports. Both methods use the same basic input: the hourly digital precipitation product (HDP) computed by each radar within the ABRFC's area, and hourly rain gauge

reports. The MAPX estimates before June 15, 1996 are derived from the NEXRAD Stage III, and those thereafter are derived from either the Stage III or P1. Choice of the Stage III or P1 algorithm is dependent on the personnel at the ABRFC.

Stage III was created by the Office of Hydrology's Hydrologic Research Laboratory (HRL). It is a merged radar-gage precipitation field design to provide the spatial resolution of radar data while preserving the precipitation accumulations measured by gages (Shedd and Smith, 1991; Seo et al., 1995; Finnerty et al., 1997). In this process, the raw reflectivity data produced from the radar sites is transformed into precipitation estimates by using a standard Z-R power law relationship (Fulton, et al., 1998). The gage measurements assumed as "ground truth" are then utilized to remove a mean field bias in the radar precipitation estimates. The overlapping radar fields are merged in a gridded system known as Hydrologic Rainfall Analysis Project (HRAP) to generate the Stage III products (Greene and Hudlow, 1982).

Process 1 (P1) is developed by Brian McCormick at the US Army Corps of Engineers (COE), Tulsa District (Schmidt, et al. 2000). It has many of the same features of Stage III, including editing or removing the bad gages, inserting pseudo gages, and removing anomalous propagation. However, P1 calculates a unique bias for each grid cell rather than Stage III's single bias per radar. Basically P1 makes a contour map of the rainfall from reporting gages and adjusts the raw mosaiced radar field accordingly. A mosaic of all the hourly HDPs are created by combining them into one product that covers the entire ABRFC basin. Where radar fields overlap, the average value is taken. A collection of all hourly

reporting rainfall amounts from gauge sites is also created. An irregular triangulated grid field is created by using the locations of the gauge sites. The radar mosaic is overlaid on this triangulated grid and a bias field is created based on the difference between the radar field value and the gauge field value. Where there is no gauge site, a bias is computed using the triangular grid and the distance from the nearest gauge sites. The resultant bias field is then used to create the final precipitation product.

Another important step involved in radar data processing procedure is the data adjustment when the bias is too large with comparison to real-time rain gage data on an hourly time step (Fulton, et al., 1996). This adjustment is done through an automated, objective tuning of the multiplicative coefficient in the Z-R relationship. The adjustment is often made for winter seasons due to snow cover caused more reflectivity of radar beam. Therefore, the radar estimates during winter should be relatively close to the gauged data. However, such an adjustment is rarely made in ABRFC due to a few snow events.

1-hr MAPH data are derived from a historic network of precipitation gages, which is operated by the NCDC. 63 rain gages over the study region were selected to compute MAPH. The weight for each station was determined by the Thiessen polygon method. Quality control procedures are applied not only to the raw data but also at various stages of calculation process. The most important check is the effects of man-made changes to the station, such as relocation of station, equipment changes. Effects of these man-made changes

are reduced by the implementation of a graphical interactive procedure called the Interactive Double Mass Analysis (IDMA).

In this study, the 1-hr MAPX and 1-hr MAPH are summed to derive a 6-hr MAPX and MAPH so that the three MAPs were in the same time step. Analyses are conducted based on these 6-hr MAP and MAPX values. For the comparison analyses of MAPX, MAPO and MAPH, the missing data as well as their matched mates are removed.

3. **RESULTS AND ANALYSIS**

For statistical evaluation of the radar-based MAPX in comparison to gauged MAPs, the following criteria are selected:

The Mean Bias

$$ME = \frac{1}{N}\sum_{i=1}^{N}(R_i - G_i)$$

The Mean Relative Bias

$$MRE = \frac{\frac{1}{N}\sum_{i=1}^{N}(R_i - G_i)}{\frac{1}{N}\sum_{i=1}^{N}G_i}$$

Where R_i is a radar-based MAPX value, G_i is a gauge-based MAP value, N is the number of the values.

3.1 **Overall Evaluation**

In general, the MAPX values are in very good agreement with the MAPO and MAPH for most of the basins. This is borne out by analyzing the long-term 6-hr average of MAPX, MAPO and MAPH, which are listed in Table 2. The overall ratio of MAPX to MAPO and MAPH shows that MAPX values are lower than MAPO but higher than MAPH. The basin KNSO2 had cumulative MAPX values that were slightly higher than the MAPO value, while the cumulative MAPX values over the basin TIFM7, WTTO2, and MLBA4 are in good agreement with the MAPO values over the study period. The reminder of the basins have MAPX values being lower than MAPO values at a range of 3~6%.

The long-term average ratios of MAPX to MAPO value over all eight basins are different from the findings by Smith et al. (1999), whose comparisons suggested MAPX values were systematically lower than MAPO values. The reason is that two more years data are employed in this study. The MAPX values seem to be higher since the P1 algorithm was interactively applied since June 1996.

The overall average 6-hr MAPX, MAPO and MAPH were analyzed using linear regression to evaluate the MAPX quality when precipitation was observed. Scatter plots of radar MAPX to gauged MAPO over the whole study period are shown in Figure 2. The linear regression models for all basins are also plotted in the figure. Figure 2 illustrates that

the MAPX values were smaller than MAPO values for all basins but KNSO2 when precipitation was observed by operational gages, even though the degrees of underestimation were different. Better performance was found in the basins TIFM7, TENO2, WTTO2, and MLBA4 compared to the rest of basins. The slopes of linear regression over basins JOPM7 and ELDO2 are 0.857 and 0.826 respectively, while they are greater than 0.900 over the other basins. Scatter plots of MAPH to MAPO over the study period, are shown in Figure 3, reveal that MAPH is close to MAPO only at the basin WTTO2. The worst regression existed at the basin ELDO2.

MAPX estimates were better when the precipitation was heavy as opposed to when there was light precipitation. The radar precipitation estimates were too low in light precipitation events. MAPX was often zero while MAPO was 2.5 mm or less. However, it is not these events which contribute significantly to flood we are concerned with.

3.2 **Time Series Comparison**

MAPX was under-estimated for all basins but KNSO2 from 1993 to 1996; thereafter overestimation of MAPX was found in 1997 and 1998 when compared to MAPO. The best MAPX data were in 1996 in term of mean bias. These facts are revealed by annual averaged 6-hr mean biases (defined as MAPX minus MAP) and standard deviation analysis listed in Table 3. Negative values in the table show an underestimation of MAPX while positive values imply an overestimation.

The effect of applying P1 algorithm for MAPX processing was obvious. It caused overestimation of annual averaged 6-hr MAPX for most of the basins since June 15, 1996. The 6-hr MAPX and MAPO analysis, including mean, standard deviation, coefficient of variation, and bias, before and after the P1 algorithm was applied, are shown in Table 4. The MAPX values before June 15, 1996 over most of the basins were underestimated and the only exception existed in the basin KNSO2. The relative bias for KNSO2 is positive, 6.59%, while they are negative for all other basins, varying from –2.03 to –14.12%. The relative mean bias became positive for all basins but TANO2 after June 15, 1996. The basins TIFM7 and TENO2 showed the good consistency of MAPX data, their relative mean bias were only 3.64% and 1.51%, respectively. The basin KNSO2 proved its exception by its bias being negative only in 1993. The bias standard deviation showed that the strongest variation occurred in 1994 for all basins, while the least variation appeared in 1997.

In order further to evaluate MAPX performance in time series, 12-month moving average monthly biases over the eight study basins are plotted in moving time series in Figure 4. These monthly biases are calculated by averaging the previous 12-month monthly biases. Therefore, the bias in 11/1994 is calculated by averaging monthly bias in a period of 12/1993 to 11/1994. Figure 4 also reveals that MAPX estimates were better over the basins TIFM7 and WTTO2 than the other basins. A systemic underestimation of MAPX values existed over most of the basins before summer 1996, thereafter MAPX values were overestimated. Such an underestimation before summer 1996 is not observed over basin KNSO2.

The time series analysis has revealed that the basin KNSO2 is an exception with a positive bias when using the stage III algorithm. The possible reasons include the "ground truth" gage density and Biscan Maximization (BM) procedure. KNSO2 is the smallest among the eight study basins but the "ground truth" gages are denser than the other basins. While MAPX values were systemically underestimated over the other basins, those MAPX values over KNSO2 should appear different and overestimated.

Biscan Maximization (BM) is a procedure in the pre-processing algorithm in which the higher value of reflectivity at either the first (0.5^0) or second elevation angles (1.5^0) is chosen for a particular polar grid bin during construction of the hybrid scan (Fulton et al., 1998). BM is originally used as an additional tool to minimize underestimation caused by beam blockage at the lowest elevation angle. However, it could enhance undesirable range dependent overestimation biases in the range interval of approximately 50-150 km due to the intersection of the second tilt angle with the bright band (Seo et al., 1995). The basins KNSO2 and WTTO2 are located in this range interval but KNSO2 was affected more strongly due to its small area. The enhancement of MAPX estimates over WTTO2 overcame the systemic underestimation therefore its bias was relatively small.

3.3 **Monthly Evaluation**

Examination of monthly mean 6-hr bias between MAPX and MAPO), shown in Table 5, revealed that MAPX in winter (November, December, January, February, and March) were more accurate than in summer. As discussed earlier, there is an adjustment

made in MAPX for winter seasons because there is snow cover that causes more reflectivity of radar beam. Therefore, the radar estimates during winter should be relatively close to the gauged data. The basins JOPM7, TIFM7, ELDO2, TALO2, and TENO2 had this trend in terms of mean bias.

Once again, the basin KNSO2 was different from the others in monthly mean bias. The effective negative bias was found only in June, this implied that the MAPX were overestimated in the other months. The MAPX over the basins WTTO2 and MLBA4 tended to be more accurate in most of months, while the best result was found in the basin TIFM7.

The conditional average monthly precipitation for the MAPX Values is higher than MAPO values for all basins. This is borne out by this study when the conditional monthly 6-hr MAPX and MAPO were analyzed. The term "conditional" in this study is defined as the condition of the data with non-zero in both gauged MAP values and gage MAP values while the MAPX and MAPO values are not missing at the same time. The results are shown in Figure 5. The best performance was in August. Difference of 0.5-2 mm in estimates existed for all other months over the basins JOPM7, ELDO2, TALO2, and TENO2.

3.4 Streamflow Simulation

In order to evaluate the hydrological effects of the three MAPs, streamflow simulations were performed using SAC-SMA model for the basin TIFM7. Parameters for the SAC-SMA were derived through manual calibration using historic gage-derived MAPH

time series during a period of Oct. 1963 and Sept. 1992. Observed mean-daily flow data were from the US Geological Survey.

Percent biases and percent RMS errors between simulated and observed runoff are presented in Table 6. The percent bias for the MAPX-forced simulation is -4.31%, while the percent bias statistic for the MAPO- and MAPH-forced simulations is -8.79% and -11.72%, respectively. It is interesting to note that while the SAC-SMA model was calibrated with MAPH data for the period of 1963 to 1984, the use of MAPH data led to the worst bias statistic for the period from 1993 to 1997.

We offer two related explanations for this. First, the period for the statistics in Table 6 is very short compared to the period of calibration. This short period may be dominated by underestimation of MAPH compared to MAPO in the summer convective season. Second, Figure 1 shows that the historical gage network seems to be sparse compared to the operational gage network. While the historical gage network contains only one gage in the basin interior, near the western edge, the operational network contains a gage near the center of the basin. This difference in gage coverage seems to lead to different average daily values for MAPO and MAPH in the summer months. For the months of June and July, the daily historic MAP values are about 25% less than the daily operational MAP values.

Analysis of the largest event of this period, in June, 1995, seems to support these two explanations. When this event is removed from the computation of comparison statistics, the percent bias values in Table 6 for MAPX, MAPO, and MAPH-forced simulations change to -

4.90%, -8.22%, and -8.76%, respectively. For this event, the MAPH, MAPO, and MAPX storm total precipitation values are 1.55 in., 2.43 in., and 3.31 in., respectively. These storm totals indicate that the event was spatially variable and that only the radar was able to capture an accurate estimate of the total volume of precipitation. The plot of observed and simulated hydrographs for this event shown in Figure 6 reveals that the MAPX-forced simulation is superior to both gage-based simulations, supporting the findings of Johnson, et al. (1999).

4 CONCLUSIONS

The radar-based MAPX values are in very good agreement with the gauged MAPs for most of the study basins. The overall ratio of MAPX to MAPO for all eight basins is 1.004. The long-term MAPH values is lower than MAPO, its average ratio over eight basins is 0.974. Time series analysis has revealed that MAPX estimates are strongly affected by processing algorithms. The Stage III tends to underestimate MAPX while a mixed use of P1 and Stage III tends to overestimate them. Therefore, the underestimation of MAPX in a range of 3~6% was observed for all basins but KNSO2 from 1993 to 1996, thereafter overestimation of MAPX was found in years 1997 and 1998. The basin KNSO2 showed its exception by its bias being negative only in 1993.

The conditional analysis has revealed that the MAPX values were underestimated for all basins when precipitation was observed. Better performance was found in the basins TIFM7, TENO2, KNSO2, WTTO2, and MLBA4 than in the rest of basins. The slopes of linear regression over basins JOPM7 and ELDO2 are 0.857 and 0.826 respectively, while

they are greater than 0.900 over the other basins. MAPX estimates were better when the precipitation was heavy as opposed to when there was light precipitation. The radar precipitation estimates were too low in light precipitation events.

The MAPX in winter (November, December, January, February, and March) were more accurate than in summer due to the adjustment made in MAPX for winter seasons. The basins JOPM7, TIFM7, ELDO2, TALO2, and TENO2 had this trend in terms of mean bias.

The MAPX-forced simulation to produce runoff is far better than both MAPO and MAPH-forced simulation. The MAPX, MAPO and MAPH-forced simulations are with percent bias of –4.90%, –8.22% and –8.76. However, this fact is only for the short study period.

5. AKNOWLEGEMENT

The authors wish to recognize those employees at the NOAA-Office of Hydrology dedicated to making suggestion and comments on the result analysis. Special appreciation is extended to D.J. Seo, Rechard Fulton, Jay Briedenbach, Dennis Miller and Paul Tilles, Hydrologic Research Laboratory, NOAA, and Bill Lawrence, ABRFC.

REFERENCES

Borga, M., Anagnostou, E.N., and Frank, E., 1998. "On the use of real-time radar rainfall estimates for flood prediction in mountainous basins", Submitted to *J. of Geographical Research-Atmospheres.*

Burnash, R.J.C., Ferral, R.L., and McGuire, R.A., 1973. "A generalized streamflow simulation system - conceptual modeling for digital computers," U.S. Department of Commerce, National Weather Service and State of California, Department of Water Resources.

Finnerty, B., M. Smith, D.J., Seo, V. Koren, and G. Moglen, 1997: Space time scale sensitivity of the Sacramento model to radar-gauge precipitation inputs. *J. Hydrol.*, **102**, 69-92.

Fread, D., and coauthors, 1995: Modernization in the National Weather Service river and flood program. *Wea. Forecasting*, **10**, 477-484.

Fulton, R.A., Breidenbach, J.P, Seo, D.J., and Miller, D.A. Seo, D.J., and Smith, J.A., 1996. "Characterization of climatological variability of mean areal rainfall through fractional coverage," Water Resources Research, 33(7): 2087-2095.

Fulton, R.A., Breidenbach, J.P., Seo, D.J., Miller, D.A., and O'Bannon, T., 1998: The WSR-88D Rainfall Algorithm, *Weather and Forecasting*, **13**, 377-395.

Greene, D.R., and Hudlow, M.D., 1982: "Hydrometeorological grid mapping procedures." *AWRA Int. Symp. Hydrometeorology*, AWRA, Bethesda, MD.

Hudlow, M., 1988: Technological developments in real-time operational hydrological forecasting in the United states. *J. Hydrol.*, **102**, 69-92.

Seo, D.J., R. Fulton, J. Breidenbach, D. Miller, and E. Friend, 1995: Final report. Interagency Memorandum of Understanding among the NEXRAD Program, WSR-88D Operational Support Facility, and the NWS/OH Hydrologic Research Laboratory, 51 pp.

Shedd, R.C., and Smith, J.A., 1991. "Interactive precipitation processing for the modernized National Weather Service," Preprints, Seventh International Conference on Interactive Information and Processing Systems for Meteorology, Oceanography, and Hydrology, New Orleans, Louisiana, American Meteorological Society, pp. 320-323.

Smith, J.A., Seo, D.J., Baeck, M.L., and Hudlow, M.D., 1996. "An intercomparison study of NEXRAD precipitation estimates," Water Resources Research, 32(7): 2035-2045.

Smith, M., V. Koren, B. Finnerty, and D. Johnson, February 1999: Distributed Modeling: Phase I Results. NOAA Technical Report NWS 44.

Stellman, K., H. Fuelburg, R. Garza and M. Mullusky,
Vieux, B.E., and Bedient, P., 1998. "Estimation of rainfall for flood prediction from WSR-88D reflectivity: A case study, 17-18 October 1994". *Weather and Forecasting*, **Vol.** 13, **No.** 2, 407-415.

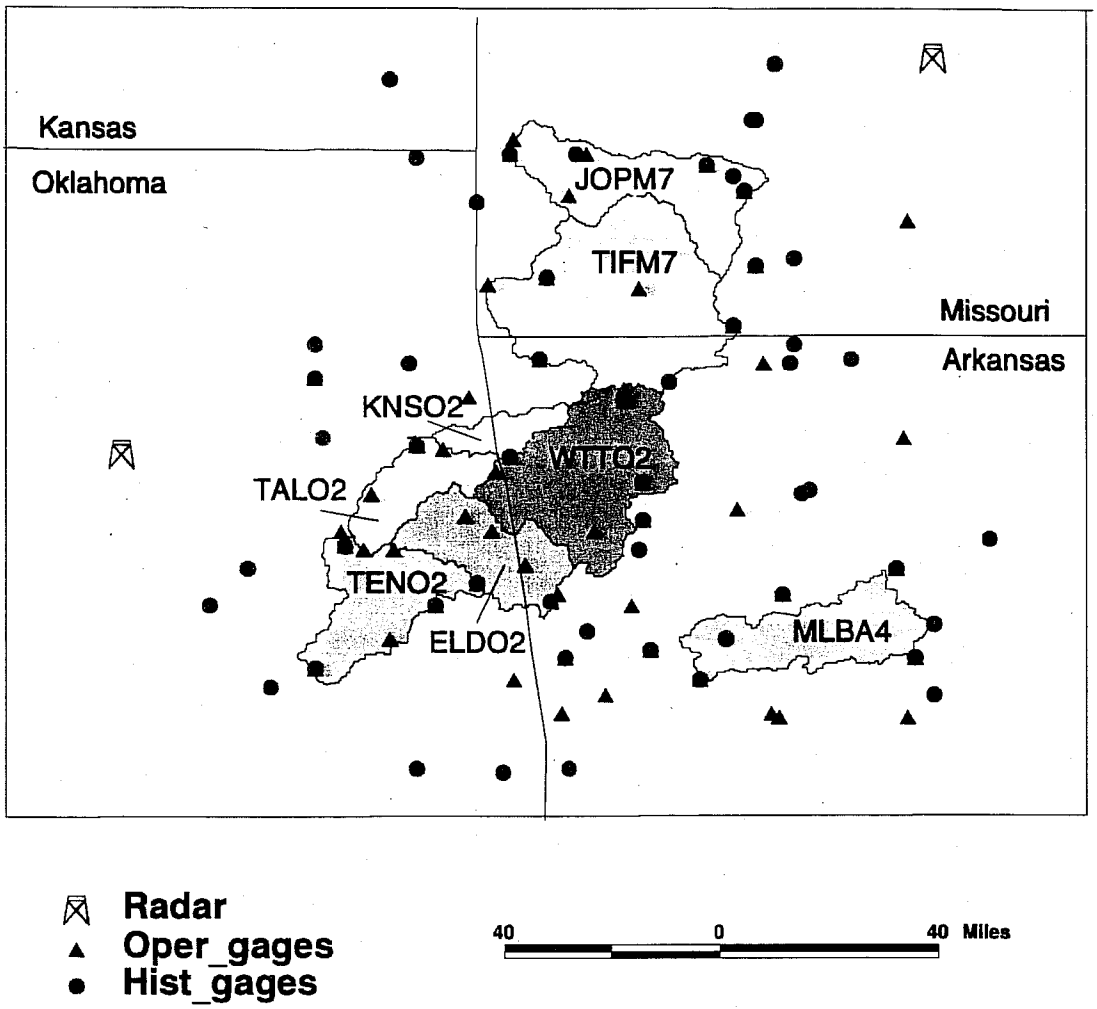

Figure 1. Location map of study basins showing radar locations, operational and historic gauges.

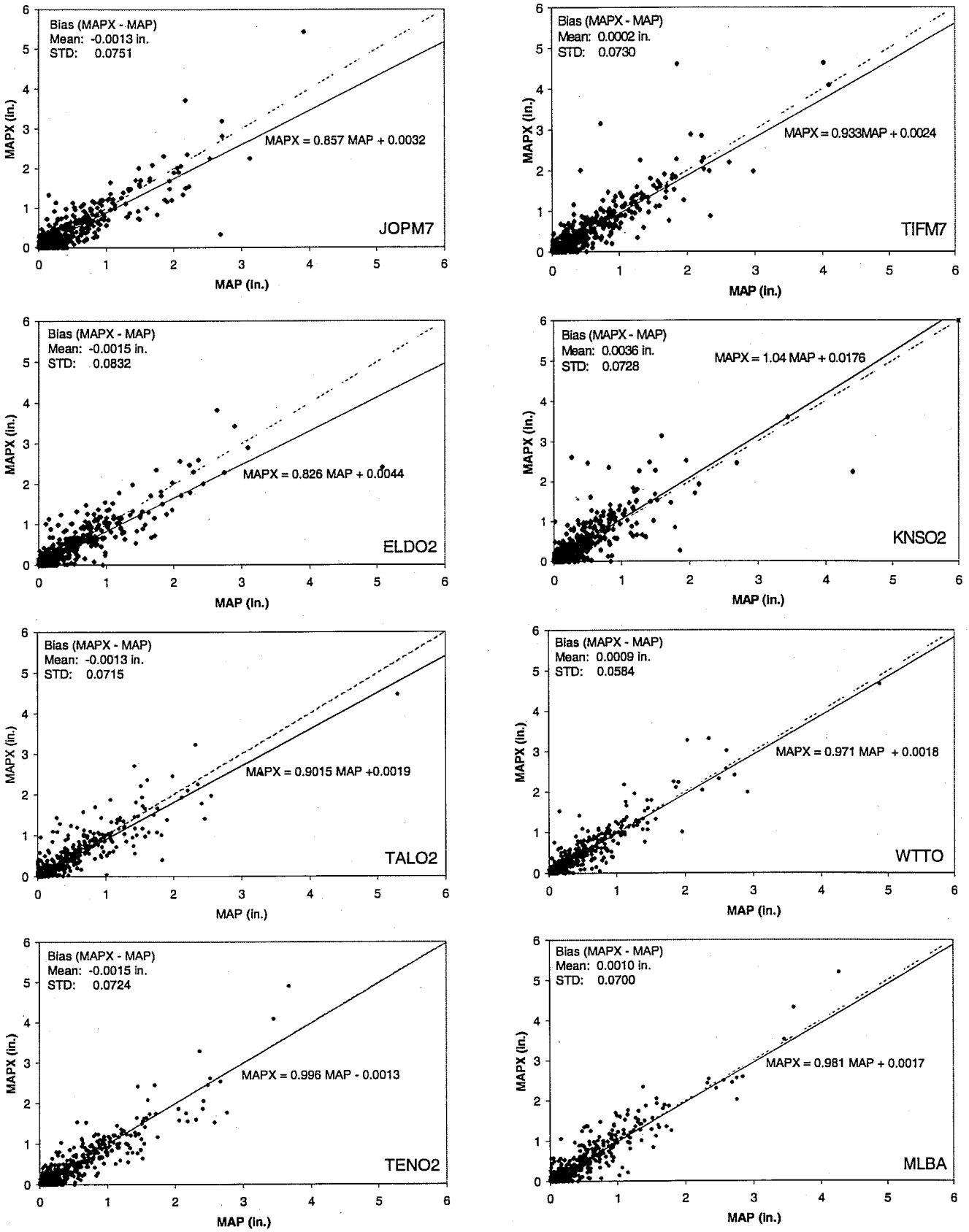

Figure 2. Scatter plot of overall 6-h MAPX to MAP over the eight study basins. The linear regression of MAPX vs MAP is plotted in solid line while 1:1 ratio line is plotted in dashed.

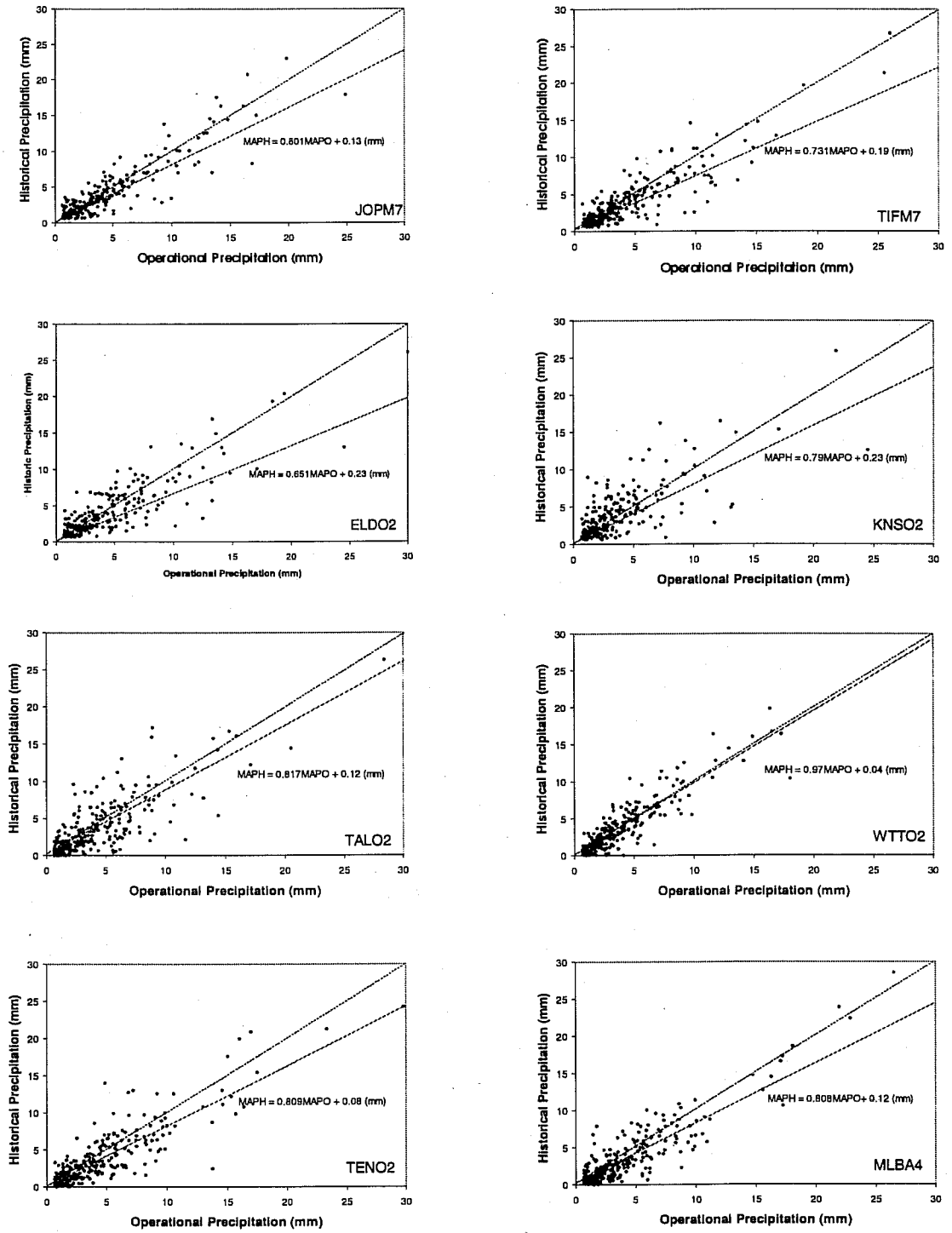

Figure 3. Scatter plot of overall 6-h MAPH to MAPO over the eight study basins. The linear regression of MAPH vs MAPO is plotted in solid line while 1:1 ratio line is plotted in dashed.

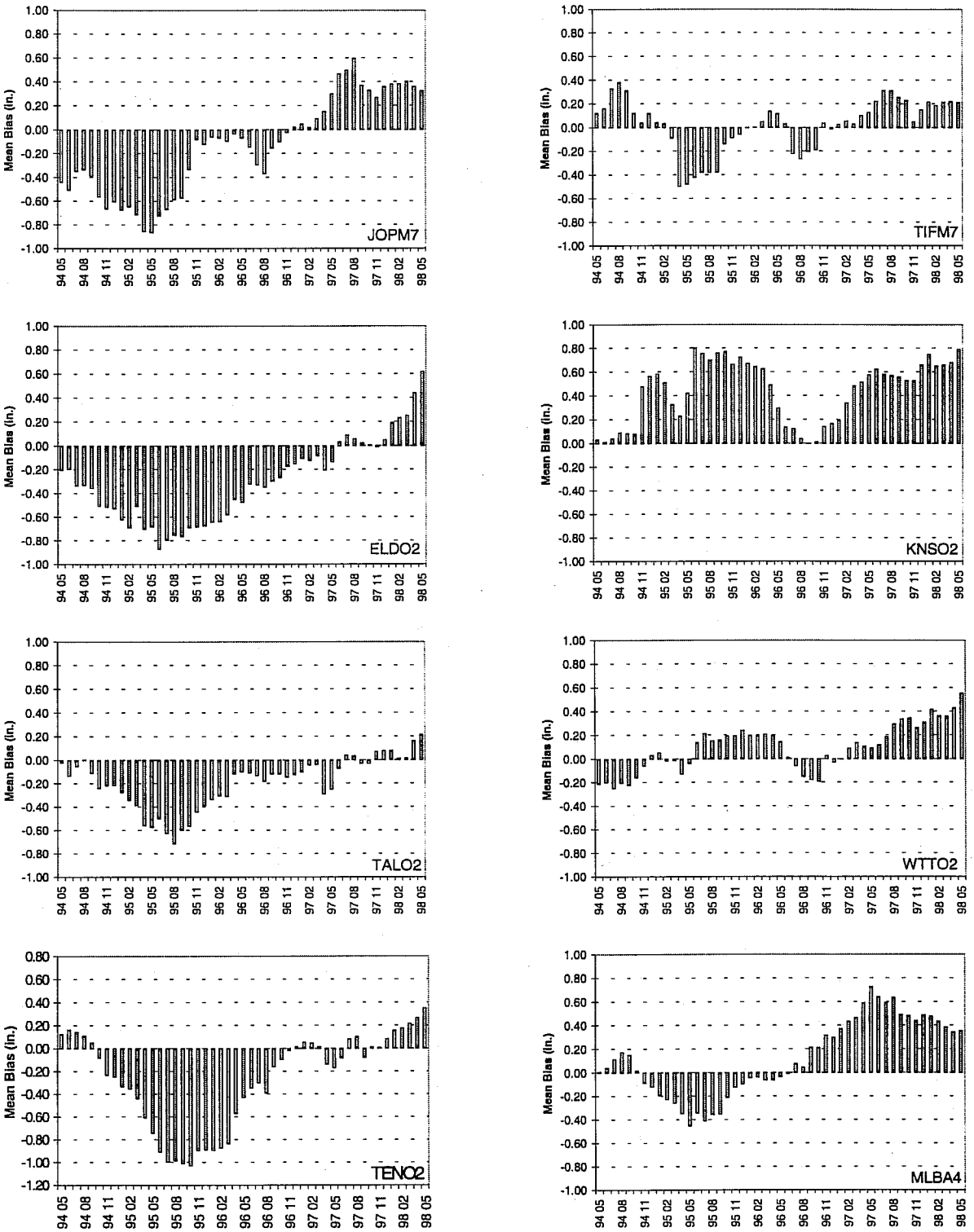

Figure 4. 12-month moving average monthly bias between MAPX and MAPO over the eight study basins.

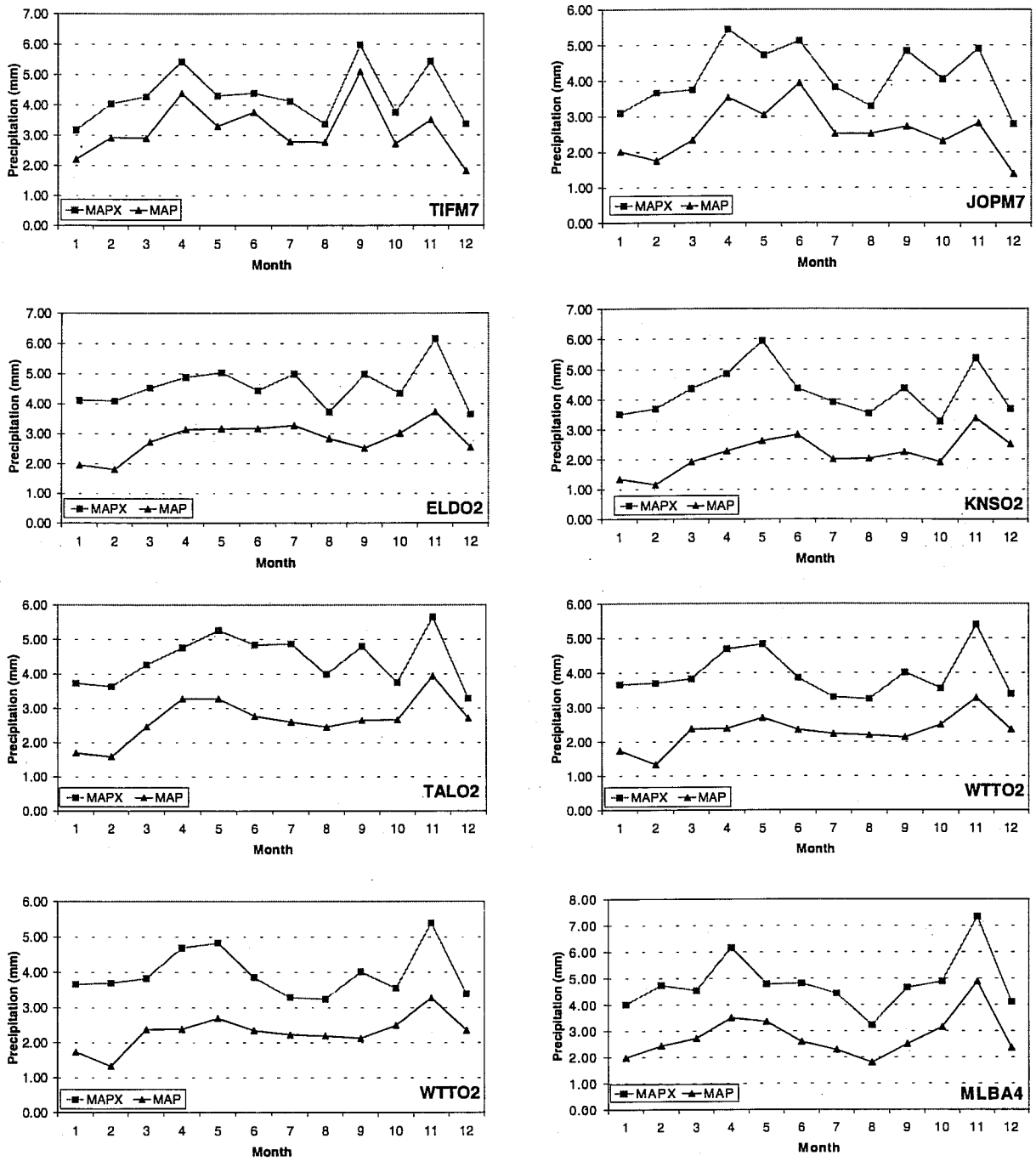

Figure 5. Conditional monthly 6-h MAPX and MAPO values over the eight study basins.

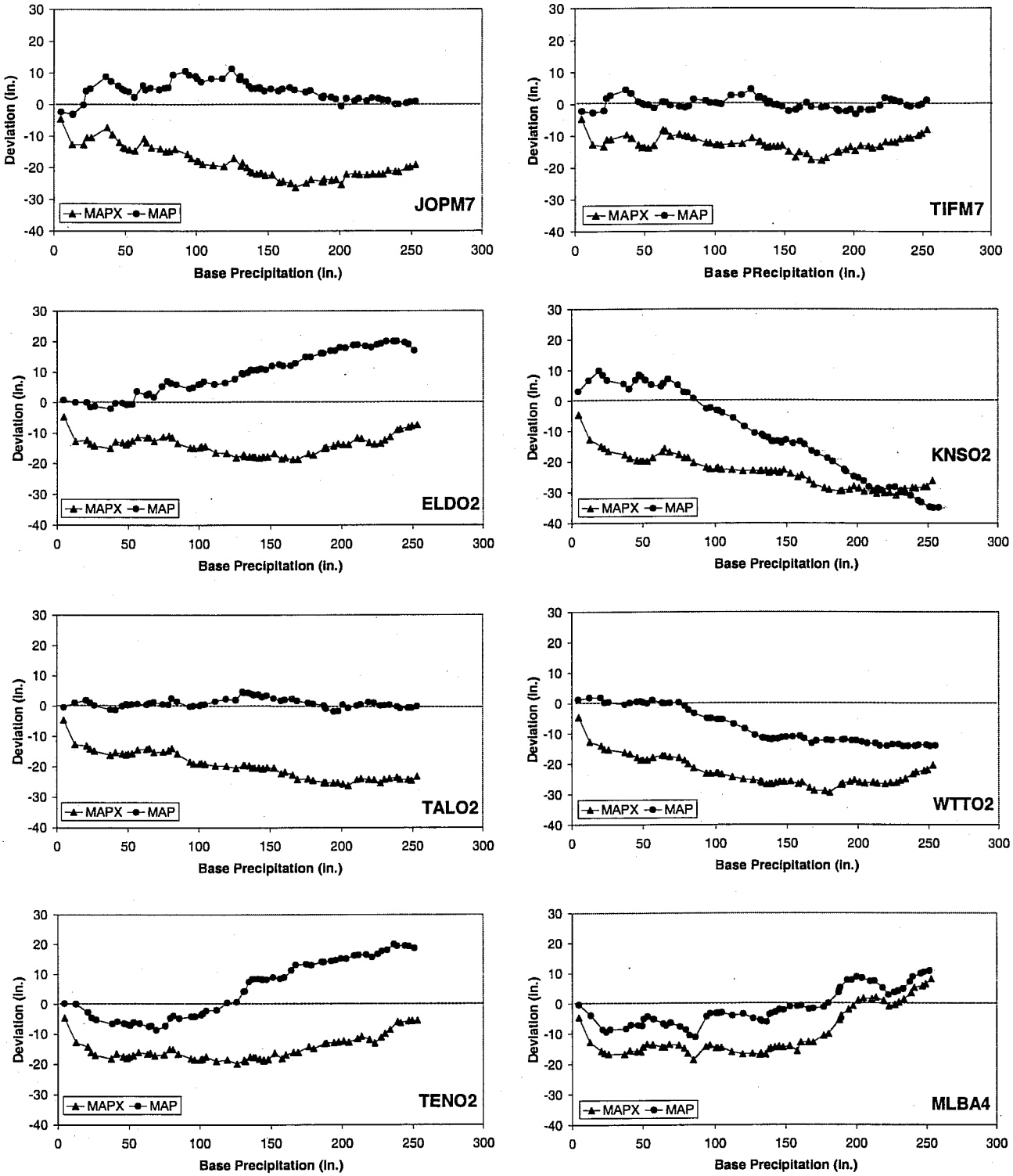

Figure 6. Consistency comparison of MAPX and MAP over the eight basins. Y-axle in figure is deviation of MAPs from its base precipitation.

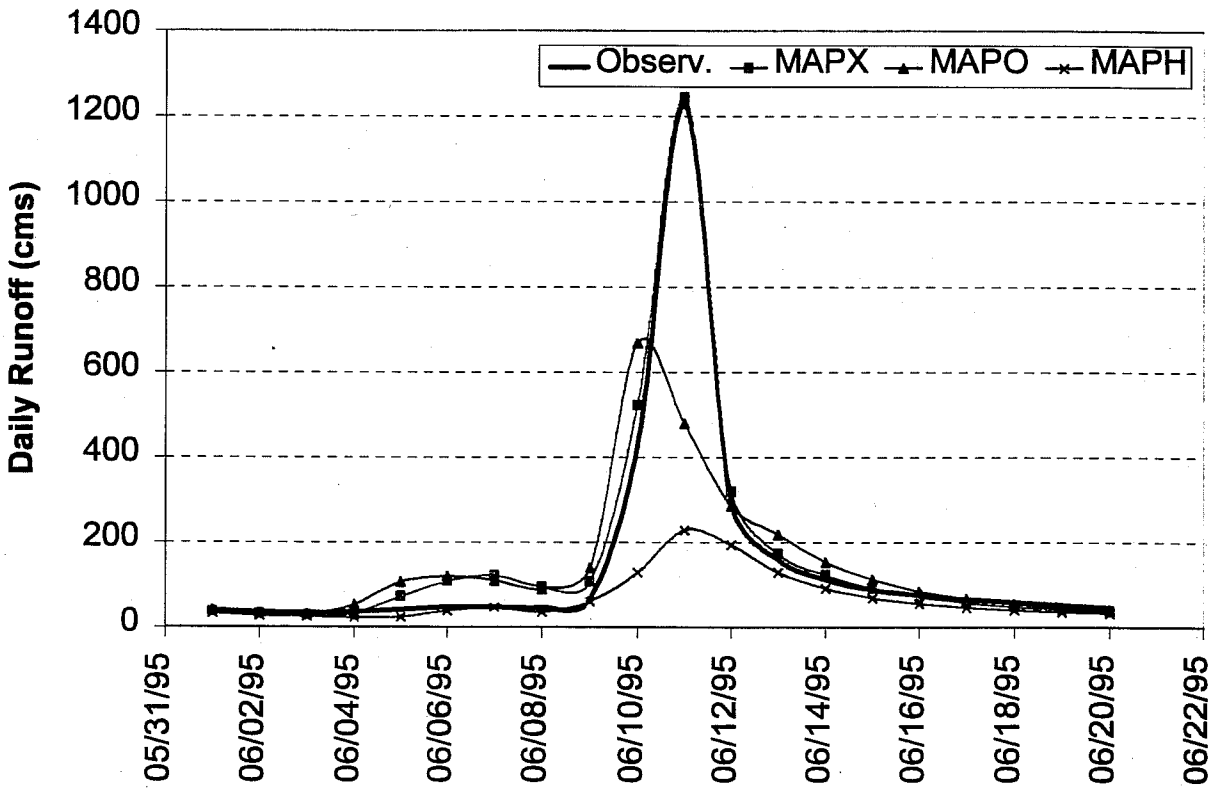

Figure 7. Simulated and observed hydrograph for event of June 1995.

Table 1. Characteristics of eight sub-basins in Arkansas-red River Basin

No.	Basin Name	Lat./Long. Centroid	Area (km^2)
1	Eldon, OK (ELDO2)	35.91/94.59	795
2	Tenkiller, OK (TENO2)	35.79/94.88	894
3	Watts, OK (WTTO2)	36.12/94.32	1645
4	Kansas, OK (KNSO2)	36.23/94.58	285
5	Tahlequah, OK(TALO2)	36.08/94.78	552
6	Joplin, MO (JOPM7)	36.90/94.25	1106
7	Tiff City, MO (TIFM7)	35.60/94.25	2259
8	Mulberry, AR (MLBA4)	35.69/93.72	1103

Table 2. The average 6-hr of MAPX, MAPO and MAPH as well as their over the eight study basins for the period of June 1, 1993 to May 31, 1998

BASIN	Average 6-hr Precipitation (mm)			Longterm Precipitation Ratio		
	MAPX	MAPO	MAPH	MAPX/MAPO	MAPX/MAPH	MAPH/MAPO
JOPM7	0.759	0.803	0.773	0.945	0.983	0.962
TIFM7	0.844	0.848	0.809	0.995	1.043	0.954
KNSO2	0.743	0.666	0.773	1.116	0.962	1.160
ELDO2	0.814	0.882	0.803	0.923	1.014	0.911
TALO2	0.764	0.803	0.780	0.952	0.979	0.972
WTTO2	0.760	0.751	0.772	1.011	0.983	1.028
TENO2	0.826	0.878	0.793	0.941	1.041	0.903
MLBA4	0.860	0.837	0.800	1.027	1.075	0.955
Average	0.796	0.809	0.788	0.985	1.011	0.974

Table 3. Annual 6-h mean bias (mm) and standard deviation between MAPX and MAPO over the eight study basins

Year	TALO2		ELDO2		JOPM7		TIFM7		KNSO2		WTTO2		TENO2		MLBA4	
	MEAN	STD	MEAN	STD	MEAN	STD	MEAN	STD	MEAN	STD	MEAN	STD	MEAN	STD	MEAN	STD
93	-0.0030	0.0910	-0.0019	0.0882	-0.0103	0.0899	-0.0041	0.0654	-0.0089	0.0933	-0.0067	0.0674	-0.0008	0.0570	-0.0017	0.0582
94	-0.0019	0.1030	-0.0047	0.1329	-0.0054	0.1098	0.0010	0.0947	0.0050	0.1013	0.0003	0.0643	-0.0022	0.0786	-0.0011	0.0653
95	-0.0032	0.0686	-0.0056	0.0736	-0.0010	0.0579	-0.0005	0.0912	0.0059	0.0774	0.0020	0.0593	-0.0073	0.0641	-0.0008	0.0789
96	-0.0010	0.0483	-0.0013	0.0450	0.0002	0.0618	-0.0001	0.0564	0.0014	0.0434	-0.0003	0.0614	0.0001	0.0931	0.0025	0.0801
97	0.0006	0.0509	0.0004	0.0521	0.0030	0.0624	0.0012	0.0493	0.0054	0.0493	0.0025	0.0447	0.0007	0.0577	0.0040	0.0688
98	0.0016	0.0558	0.0107	0.0866	0.0033	0.0514	0.0038	0.0552	0.0099	0.0612	0.0072	0.0522	0.0044	0.0667	0.0023	0.0388

Table 4. Statistical analysis using 6-hr MAPX and MAPO values when precipitation was observed by operational gages before June 15, 1996.

BAISN	6-h Mean (mm)		6-h STD (mm)		6-h Coef. of Varia.		Bias	
	MAPO	MAPX	MAPO	MAPX	MAPO	MAPX	Mean(mm)	%
JOPM7	0.1196	0.1027	0.2468	0.2272	2.06	2.21	-0.0169	-14.12
TIFM7	0.1282	0.1237	0.2460	0.2638	1.92	2.13	-0.0045	-3.51
WTTO2	0.0929	0.0910	0.1966	0.2119	2.12	2.33	-0.0019	-2.03
KNSO2	0.0902	0.0961	0.1918	0.2187	2.13	2.27	0.0059	6.59
ELDO2	0.1127	0.0985	0.2614	0.2295	2.32	2.33	-0.0142	-12.64
TALO2	0.1026	0.0945	0.2133	0.2271	2.08	2.40	-0.0080	-7.82
TENO2	0.1295	0.1163	0.2428	0.2558	1.87	2.20	-0.0132	-10.23
MLBA4	0.1044	0.0989	0.2280	0.2411	2.18	2.44	-0.0055	-5.27

Table 5. Statistical analysis using 6-hr MAPX and MAPO values when precipitation was observed by gages after June 15, 1996.

BAISN	6-h Mean (mm)		6-h STD (mm)		6-h Coef. of Varia.		Bias	
	MAPO	MAPX	MAPO	MAPX	MAPO	MAPX	Mean(mm)	%
JOPM7	0.0846	0.0906	0.2067	0.2375	2.44	2.62	0.0060	7.15
TIFM7	0.1237	0.1282	0.2480	0.2724	2.01	2.12	0.0045	3.64
WTTO2	0.0861	0.0926	0.2080	0.2282	2.42	2.46	0.0066	7.64
KNSO2	0.0795	0.0959	0.1846	0.2227	2.32	2.32	0.0163	20.53
ELDO2	0.1092	0.1156	0.2789	0.2967	2.55	2.57	0.0064	5.86
TALO2	0.1081	0.1067	0.2286	0.2438	2.11	2.28	-0.0014	-1.26
TENO2	0.1205	0.1223	0.2626	0.3245	2.18	2.65	0.0018	1.51
MLBA4	0.1155	0.1260	0.2288	0.2733	1.98	2.17	0.0105	9.09

Table 6. Monthly 6-h mean bias (mm) and its standard deviation between MAPX and MAPO over the eight study basins

Month	JOPM7		TIFM7		KNSO2		ELDO2		TALO2		WTTO2		TENO2		MLBA4	
	MEAN	STD	MEAN	STD	MEAN	STD	MEAN	STD	MEAN	STD	MEAN	STD	MEAN	STD	MEAN	STD
1	0.0013	0.0452	0.0036	0.0544	0.0069	0.0630	0.0039	0.0852	0.0033	0.0597	0.0046	0.0670	0.0017	0.0521	-0.0029	0.0392
2	0.0009	0.0375	0.0018	0.0293	0.0068	0.0517	0.0016	0.0423	0.0017	0.0342	0.0033	0.0336	0.0005	0.0273	0.0031	0.0437
3	0.0043	0.0556	0.0050	0.0581	0.0087	0.0862	-0.0024	0.1697	0.0001	0.0728	0.0006	0.0667	0.0024	0.0605	-0.0002	0.0610
4	-0.0009	0.0907	0.0017	0.0964	0.0076	0.0672	-0.0009	0.0723	-0.0047	0.0768	0.0034	0.0529	-0.0001	0.0723	0.0009	0.0584
5	0.0003	0.0554	-0.0011	0.0623	0.0059	0.0783	0.0004	0.0731	-0.0002	0.0564	0.0035	0.0630	-0.0014	0.0741	0.0005	0.0830
6	-0.0074	0.1072	-0.0044	0.1332	-0.0026	0.1311	-0.0047	0.1101	-0.0037	0.1131	0.0015	0.0857	-0.0044	0.0733	0.0073	0.0918
7	-0.0041	0.0864	-0.0025	0.0890	0.0029	0.0634	-0.0049	0.0660	-0.0028	0.0756	0.0009	0.0519	-0.0054	0.0937	0.0044	0.0701
8	-0.0026	0.0718	-0.0033	0.0492	0.0013	0.0491	-0.0067	0.0529	-0.0018	0.0639	-0.0046	0.0553	-0.0070	0.0863	0.0016	0.0659
9	0.0004	0.0655	-0.0041	0.0449	0.0013	0.0632	-0.0019	0.0454	-0.0014	0.0942	-0.0017	0.0562	-0.0013	0.1225	0.0030	0.1035
10	-0.0051	0.1237	-0.0011	0.0817	0.0020	0.0384	-0.0033	0.0612	-0.0008	0.0490	-0.0022	0.0475	0.0007	0.0634	-0.0024	0.0824
11	-0.0031	0.0693	0.0027	0.0690	0.0031	0.0892	0.0007	0.0825	-0.0027	0.0915	0.0023	0.0675	-0.0039	0.0726	-0.0019	0.0803
12	0.0004	0.0382	0.0038	0.0454	-0.0007	0.0504	-0.0001	0.0363	-0.0024	0.0358	-0.0004	0.0341	-0.0001	0.0312	0.0000	0.0316
Totally	-0.0013	0.0751	0.0002	0.0730	0.0036	0.0728	-0.0015	0.0832	-0.0013	0.0715	0.0009	0.0584	-0.0015	0.0724	0.0010	0.0700

Table 7. Percent Biases and Percent RMS in Monthly Volumes Simulated by SAC-SMA by using Three MAP Time Series.

	Percent Bias %			Percent RMS %		
Month	RADAR	OPER.	HIST.	RADAR	OPER.	HIST.
October	-15.81	-7.83	-8.84	34.34	23.59	27.16
November	-4.18	-0.39	30.8	82.5	72.21	62.18
December	-2.41	-27.32	-28.17	52.66	34.52	29.77
January	-0.12	0.98	3.93	46.16	58.99	35.1
February	-13.24	-27.72	-23.21	37.02	32.75	25.59
March	-2.09	-27.68	-12.78	30.43	57.68	23.57
April	34.5	13.02	6.74	52.43	53.29	8.39
May	5.16	-3.78	2.2	12.72	13.63	24.16
June	-32.11	-32.2	-59.43	65.72	63.69	89.36
July	-68.28	-46.32	-54.23	126	84.66	88.92
August	-42.45	-27.02	-43.21	66.67	67.13	60.92
September	-16.63	12.54	-35.64	22.62	41.15	52.4
Year Avg.	-4.90	-8.22	-8.76	66.82	63.95	58.94